

117 The development of fatal AIH was initiated at 2 weeks of  
 118 age, and extensive destruction of the liver parenchyma  
 119 resulted in most mice dying by 4 weeks. Fatal AIH in  
 120 BALB/c-NTx-PD-1<sup>-/-</sup> mice was characterized by CD4<sup>+</sup>  
 121 and CD8<sup>+</sup> T-cell infiltration with massive lobular  
 122 necrosis in the liver, hypergammaglobulinemia, and pro-  
 123 duction of ANA.<sup>11,12</sup> In BALB/c-NTx-PD-1<sup>-/-</sup> mice, fatal  
 124 AIH was initiated at 2 weeks by splenic follicular helper T  
 125 (T<sub>FH</sub>) cells, powerfully assisting B cells in forming  
 126 germinal centers (GCs).<sup>13</sup> In addition, these T<sub>FH</sub> cells  
 127 in the spleen directly migrated into the liver via the  
 128 CCR6-CCL20 axis, triggering the induction of AIH.<sup>12</sup>  
 129 However, the development of mouse models of chronic  
 130 hepatitis similar to the human disease remains an  
 131 important challenge.

132 In the present study, using our mouse model of fatal  
 133 AIH, we examined the effects of administering dexa-  
 134 methasone (DEX) versus splenectomy on the development  
 135 or progression of AIH. In addition, we developed a new  
 136 model of chronic AIH. NTx-PD-1<sup>-/-</sup> mice on the different  
 137 genetic background C57BL/6 developed chronic hepatitis  
 138 with fibrosis, hypergammaglobulinemia, and the produc-  
 139 tion of ANA, allowing us to examine the effects of  
 140 administering DEX versus splenectomy.

## 142 Materials and Methods

143 All protocols for mice, administration of DEX in vivo,  
 144 histological and immunohistological analysis, flow cytometry  
 145 analysis, isolation of lymphocytes, enzyme-linked immunosor-  
 146 bent assay, adoptive transfer, and histological activity index  
 147 (HAI) scores<sup>14</sup> are detailed in Supplementary Materials  
 148 and Methods.

## 150 Statistical Analysis

151 The data are presented as the mean values ± standard  
 152 deviation (SD). Statistical analysis was performed by Student  
 153 *t* test for unpaired data to compare the values between the 2  
 154 groups, and variance was analyzed with the Tukey-Kramer test  
 155 for multiple comparisons. Survival rates were estimated by the  
 156 Kaplan-Meier method and compared with the log-rank test.  
 157 *P* values less than .05 were considered significant.

## 158 Results

### 159 DEX Prevents the Development of Fatal AIH 160 in BALB/c-NTx-PD-1<sup>-/-</sup> Mice

161 First, to determine whether corticosteroid therapy  
 162 prevents AIH in BALB/c-NTx-PD-1<sup>-/-</sup> mice, starting 1 day  
 163 after thymectomy, the mice were treated intraperitoneally  
 164 every other day with DEX diluted in phosphate-buffered  
 165 saline (PBS) or with PBS alone (Figure 1A). After 13  
 166 injections, mice at 4 weeks of age showed that DEX  
 167 suppressed severe infiltration of mononuclear cells as well  
 168 as massive destruction of the liver parenchyma with  
 169 decreased serum concentrations of aspartate aminotrans-  
 170 ferase (AST) and alanine aminotransferase (ALT), result-  
 171 ing in a significantly higher survival rate compared  
 172 with control PBS injections (Figure 1A and B and

173 Supplementary Figure 1A). These data indicate that DEX  
 174 prevents fatal AIH in these mice.

### 175 Therapeutic Administration of DEX Induces 176 Regression of Inflammation in the Liver 177 and Significantly Increases Survival in 178 BALB/c-NTx-PD-1<sup>-/-</sup> Mice

179 Next, we examined whether corticosteroids might  
 180 have the same therapeutic efficacy for AIH in BALB/  
 181 c-NTx-PD-1<sup>-/-</sup> mice as for AIH in humans. Because  
 182 induction of AIH was started by 14 days of age in most of  
 183 the mice,<sup>11,12</sup> intraperitoneal injections of DEX were  
 184 started at 17 days (Figure 1C). After 6 injections admin-  
 185 istered every other day, therapeutic injections of DEX  
 186 suppressed AIH, inducing significantly greater survival at  
 187 4 weeks (Figure 1C and D and Supplementary Figure 1B).  
 188 These data suggest that similar to AIH in humans, treat-  
 189 ment with corticosteroids after induction of AIH is ther-  
 190 apeutic for BALB/c-NTx-PD-1<sup>-/-</sup> mice.

### 191 Administration of DEX Reduces Serum 192 Immunoglobulin G Levels and Production 193 of ANA in BALB/c-NTx-PD-1<sup>-/-</sup> Mice

194 Using enzyme-linked immunosorbent assay (ELISA)  
 195 and immunofluorescence assay, we next examined  
 196 whether immunoglobulin (Ig) G or ANA levels were  
 197 affected by preventive or therapeutic injections of DEX.  
 198 Although serum IgM levels were not changed by treatment  
 199 with DEX, serum IgG levels were significantly reduced by  
 200 both preventive and therapeutic injections of DEX  
 201 (Figure 1E). These data are consistent with the finding in  
 202 patients with AIH that reduced serum AST level after  
 203 corticosteroid therapy is generally associated with reduced  
 204 levels of  $\gamma$ -globulin and IgG. In addition, ANA levels were  
 205 reduced significantly in mice with preventive injections  
 206 and slightly but not significantly in mice treated with  
 207 therapeutic injections of DEX (Figure 1E and F).

### 208 Therapeutic Administration of DEX Reduces 209 the Size of the Spleen But Does Not Completely 210 Regress GC-Forming B-Cell Follicles and T<sub>FH</sub> 211 Cells in the Spleen of BALB/c-NTx-PD-1<sup>-/-</sup> 212 Mice

213 As reported previously,<sup>12</sup> the spleens of BALB/  
 214 c-NTx-PD-1<sup>-/-</sup> mice at 4 weeks of age were enlarged,  
 215 showing multiple peanut agglutinin (PNA)<sup>+</sup> GC-forming  
 216 B-cell follicles. Treatment with DEX significantly  
 217 reduced spleen size and weight, suggesting that they affect  
 218 the induction site of development of AIH (Figure 2A and  
 219 Supplementary Figure 2A and B). However, therapeutic  
 220 but not preventive DEX injections allowed persistence of  
 221 multiple B-cell follicles in the spleen (Figure 2B, upper  
 222 panels) and of CD4<sup>+</sup> T<sub>FH</sub> cells as well as PNA<sup>+</sup> GC for-  
 223 mation in the B220<sup>+</sup> B-cell follicles (Figure 2B, middle and  
 224 lower panels) in the spleens of BALB/c-NTx-PD-1<sup>-/-</sup> mice  
 225 aged 4 weeks. In addition, flow cytometric analysis of splenic  
 226 CD4<sup>+</sup> T cells showed that these cells in mice therapeutically



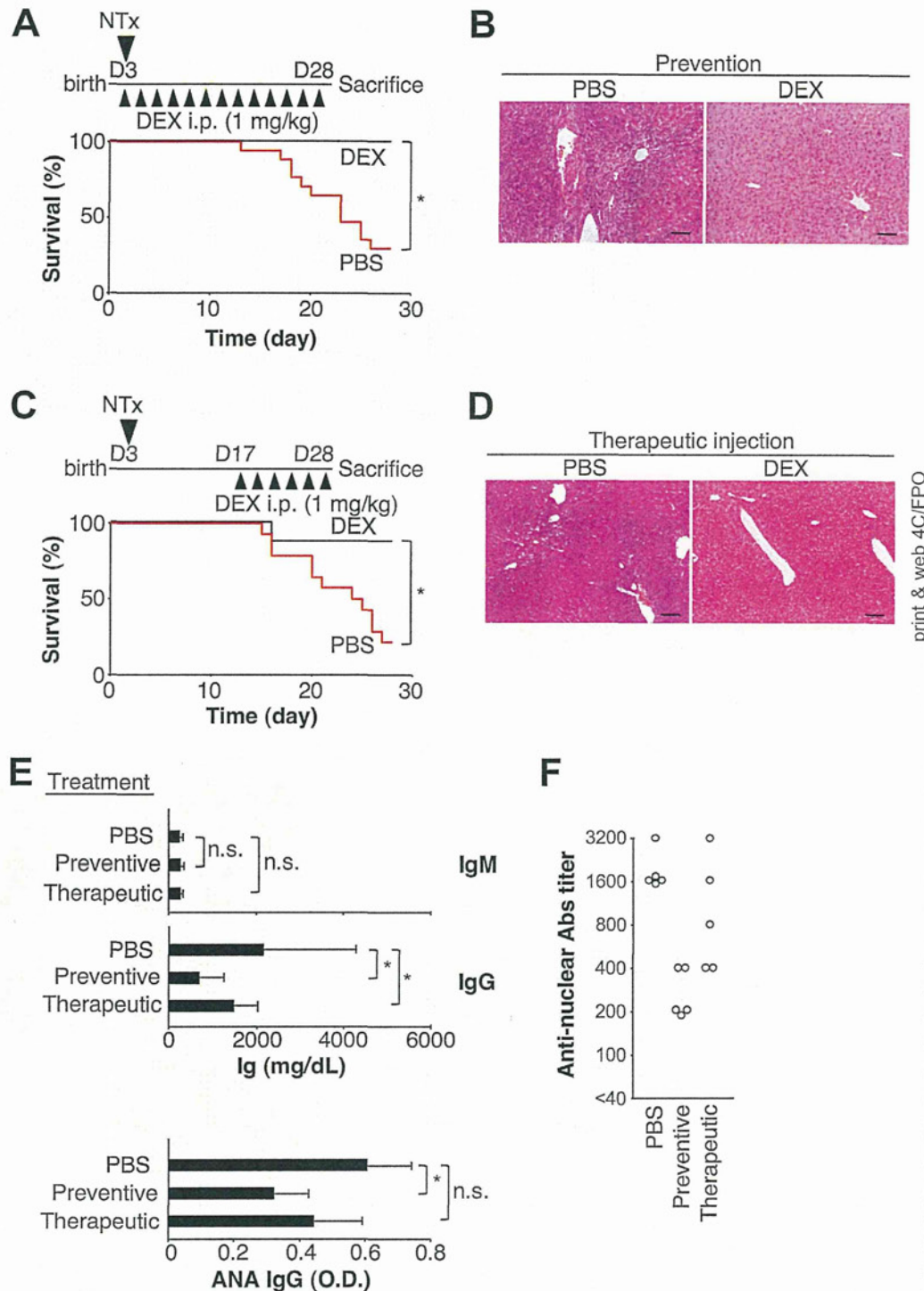


**Figure 1.** Either preventive or therapeutic injection of DEX suppressed fatal AIH in BALB/c-NTx-PD-1<sup>-/-</sup> mice. (A, B, E, F) With preventive injections, mice at 1 day after thymectomy were intraperitoneally injected every other day with 1.0 mg/kg DEX diluted in PBS (n = 5) or PBS alone (n = 17). After 13 injections, mice at 4 weeks of age were killed. (C-F) With therapeutic injections, mice at 14 days after thymectomy were injected every other day with DEX (n = 11) or PBS alone (n = 13). After 6 injections, mice at 4 weeks of age were killed. (B and D) Liver staining with H&E. (E) Serum levels of IgM, IgG, and ANA measured by ELISA. (F) Serum titers of ANAs. *Open circles* indicate the maximum dilution of sera from individual mice as detected by fluorescence immunohistology. *Bars* indicate the mean of each group, and the *error bars* indicate SD. \**P* < .05. All *scale bars* = 100 μm.

treated with DEX contained ICOS<sup>+</sup>CXCR5<sup>+</sup> T<sub>FH</sub> cells at levels similar to those of controlled mice treated with PBS. In contrast, ICOS<sup>+</sup>CXCR5<sup>+</sup> T<sub>FH</sub> cells in CD4<sup>+</sup> T-cell populations were reduced in mice preventively treated with DEX (Figure 2C). Although injections of DEX may affect immune cells other than T cells in the spleen, therapeutic injections of DEX allowed T<sub>FH</sub> cells to persist.

Corticosteroids directly induce apoptosis of lymphocytes, whereas Tregs expressing higher levels of

glucocorticoid receptors are reported to be resistant to DEX-mediated apoptosis, probably due to high expression of Bcl-2.<sup>15-17</sup> We next examined whether splenic CD4<sup>+</sup> T cells containing T<sub>FH</sub> cells are more resistant to DEX-mediated apoptosis than other T cells. CD4<sup>+</sup> and CD8<sup>+</sup> T cells were purified from the spleen of BALB/c-NTx-PD-1<sup>-/-</sup> mice therapeutically treated with DEX and cultured with various concentrations of DEX (Figure 2D). After 3 days of culture, 7-AAD<sup>-</sup> nonapoptotic



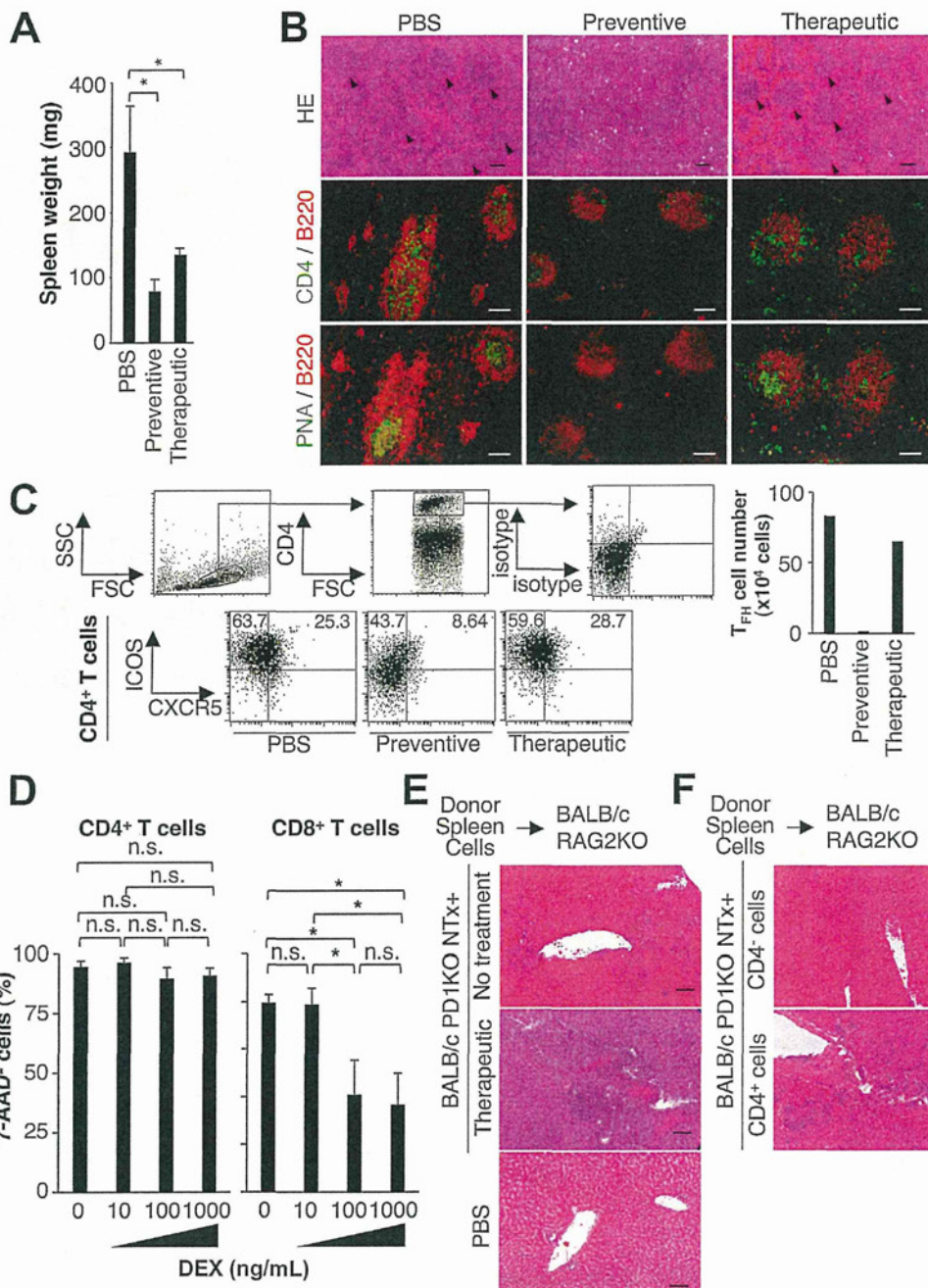


**Figure 2.** Therapeutic administration of DEX reduces spleen weight but does not completely regress T<sub>H</sub> cells in the spleen of BALB/c-NTx-PD-1<sup>-/-</sup> mice. Mice were treated with DEX or PBS alone preventively or therapeutically, as described in Figure 1. (A) Spleen weights. (B) Histological analysis of the spleens from each group with H&E staining. Arrowheads indicate follicles. Spleens from each group were immunohistologically stained for CD4, PNA (green), and B220 (red). (C) Flow cytometric analysis of splenic CD4<sup>+</sup> T cells from each group. The numbers in the plots indicate the percentage of ICOS<sup>+</sup>CXCR5<sup>+</sup> and ICOS<sup>+</sup>CXCR5<sup>-</sup> cells in the CD4<sup>+</sup> T-cell population (left panels). The numbers of ICOS<sup>+</sup>CXCR5<sup>+</sup> CD4<sup>+</sup> T (T<sub>H</sub>) cells were calculated as follows: (Percentage of Cells in Viable Cells) × (Number of Viable Cells) (right panel). (D) Flow cytometric analysis of CD4<sup>+</sup> and CD8<sup>+</sup> T cells. Spleen cells of mice injected with DEX therapeutically were cultured for 3 days with anti-CD3 and anti-CD28 monoclonal antibodies and the indicated concentration of DEX. The percentages of 7-AAD<sup>-</sup> cells in CD3<sup>+</sup>CD4<sup>+</sup> and CD3<sup>+</sup>CD8<sup>+</sup> T cells are shown. Data represent one of 3 separate experiments. (E and F) Staining with H&E of the livers from recipient BALB/c-RAG2<sup>-/-</sup> mice at 3 weeks after transfer. (E) Total splenocytes were isolated and intravenously transferred from BALB/c-NTx-PD-1<sup>-/-</sup> mice with or without therapeutic injections of DEX. (F) Purified splenic CD4<sup>+</sup> T cells or CD4<sup>+</sup> T cell-depleted splenocytes (CD4<sup>-</sup> cells) were transferred from BALB/c-NTx-PD-1<sup>-/-</sup> mice therapeutically treated with DEX. Bars indicate the mean of each group, and the error bars indicate SD. \*P < .05. n.s., not significant. Scale bars = 100 μm.

cells were significantly and dose-dependently reduced in the CD8<sup>+</sup> T-cell population cultured with DEX. In contrast, 7-AAD<sup>-</sup> nonapoptotic cells were not altered in the CD4<sup>+</sup> T-cell population cultured with DEX

(Figure 2D). These data suggest that in BALB/c-NTx-PD-1<sup>-/-</sup> mice, splenic CD4<sup>+</sup> T cells containing T<sub>H</sub> cells are more resistant to DEX-mediated apoptosis than effector CD8<sup>+</sup> T cells.



### **Residual Splenic CD4<sup>+</sup> Cells After Therapeutic Injections of DEX Can Induce Hepatitis in RAG2<sup>-/-</sup> Mice**

Next, we investigated whether residual splenic CD4<sup>+</sup> cells can induce AIH after therapeutic injections of DEX. Total splenocytes, purified splenic CD4<sup>+</sup> cells, or CD4<sup>+</sup> T cell-depleted splenocytes were transferred from BALB/c-NTx-PD-1<sup>-/-</sup> mice therapeutically treated with DEX at 3 weeks into T cell- and B cell-deficient BALB/c-RAG2<sup>-/-</sup> mice. Three weeks later, we found that transferring total splenocytes from mice therapeutically treated with DEX induced mononuclear cell infiltrations in the liver of recipient mice and significantly increased serum levels of AST and ALT to levels similar to those of untreated mice (Figure 2E and Supplementary Figure 2C). Notably, purified splenic CD4<sup>+</sup> T cells but not CD4<sup>+</sup> T cell-depleted splenocytes also induced hepatitis (Figure 2F and Supplementary Figure 2D). Taken together, these data suggest that residual splenic CD4<sup>+</sup> cells trigger the recurrence of AIH in mice after treatment with DEX.

### **Discontinuing Therapy with DEX Induces Fatal Hepatitis, Whereas Extending It Allows Residual GC-Forming B-Cell Follicles in the Spleen of BALB/c-NTx-PD-1<sup>-/-</sup> Mice**

To examine whether discontinuing treatment with DEX results in relapse, administration of DEX ended at 28 days of age after 6 therapeutic injections or continued until 40 days of age in control mice (Figure 3A). Continuous treatment with DEX maintained suppressed inflammatory infiltration in the liver and hepatic damage in association with a high survival rate (Figure 3A and B and Supplementary Figure 3), but GC-forming B-cell follicles were still present in the spleen (Figure 3B). In contrast, stopping treatment with DEX at 28 days resulted in the recurrence of hepatitis at 40 days, accompanied by reduced survival rates (Figure 3A and B and Supplementary Figure 3). These data suggest a limitation in the therapeutic use of corticosteroids for resolving the dysregulation of T<sub>FH</sub> cells in the spleen, the induction site of AIH, in BALB/c-NTx-PD-1<sup>-/-</sup> mice.

### **Splenectomy After the Development of AIH Suppresses Progression to Fatal AIH in BALB/c-NTx-PD-1<sup>-/-</sup> Mice**

Previously we reported that neonatal splenectomy has a preventive effect on the development of AIH in BALB/c-NTx-PD-1<sup>-/-</sup> mice.<sup>12</sup> In this study, we evaluated splenectomy as a therapeutic option. Similar to the neonatal procedure, splenectomy at 7 or 10 days of age before induction of AIH suppressed the development of fatal hepatitis (Figure 3C). Importantly, we found that splenectomy at 17 or 21 days of age after development of AIH also suppressed liver inflammation and improved survival, sustaining remission until 45 days (Figure 3C-E).

In addition, splenectomy at 21 days of age after treatment with DEX suppressed liver inflammation in

association with a high survival rate at 40 days of age, sustaining remission until 60 days (Figure 3F). Moreover, when we performed splenectomy at 4 weeks of age after treatment with DEX, liver inflammation was suppressed at 56 days of age (Supplementary Figure 4). These data suggest that splenectomy induces prolonged remission of AIH in BALB/c-NTx-PD-1<sup>-/-</sup> mice.

### **AIH That Develops in C57BL/6-NTx-PD-1<sup>-/-</sup> Mice Shares Characteristic Components of Chronic Hepatitis in Patients With AIH**

Clinical manifestations of AIH are varied in patients with AIH, and the disease manifestation has been associated with specific alleles of the major histocompatibility complex.<sup>1-3,18,19</sup> To test whether different genetic backgrounds induce milder disease manifestation in NTx-PD-1<sup>-/-</sup> mice, we performed NTx in PD-1<sup>-/-</sup> mice that had been backcrossed onto the C57BL/6 background for 11 generations.<sup>20</sup>

In 2-week-old BALB/c-NTx-PD-1<sup>-/-</sup> mice with hepatitis, pathogenic splenic T<sub>FH</sub> cells were preferentially localized within B220<sup>+</sup> B-cell follicles and autonomously developed PNA<sup>+</sup> GCs (Supplementary Figure 5).<sup>12</sup> In contrast, although splenic CD4<sup>+</sup> T cells were located within the follicles in C57BL/6-NTx-PD-1<sup>-/-</sup> mice of the same age, these B-cell follicles did not develop PNA<sup>+</sup> GCs (Supplementary Figure 5 and Figure 4A). Interestingly, flow cytometric analysis showed that in parallel to the increase in ICOS<sup>+</sup>CD4<sup>+</sup> T cells, including CXCR5<sup>+</sup> T<sub>FH</sub> cells, in C57BL/6-NTx-PD-1<sup>-/-</sup> mice at 6 weeks of age (Supplementary Figure 6A), PNA<sup>+</sup> GCs autonomously developed (Figure 4A) and B220<sup>+</sup> B cells expressed Fas and GL7 (Figure 4B), hallmarks of GC B cells. Importantly, livers in C57BL/6-NTx-PD-1<sup>-/-</sup> mice as young as 4 weeks showed mononuclear cell infiltrations, predominantly in the portal area. The infiltration was sustained in older mice, resulting in bridging fibrosis (Figure 4C and D *vii* and *viii* and Supplementary Figure 6B). Histological examination of the liver in 8-week-old C57BL/6-NTx-PD-1<sup>-/-</sup> mice showed interface hepatitis with periportal necrosis without bile duct destruction (Figure 4D, *i-iii*), intralobular degeneration (Figure 4D, *iv*), or portal inflammation (Figure 4D, *v*) as well as fibrosis (Figure 4D, *vi*). These findings are associated with an increased HAI score and increased serum levels of AST and ALT (Figure 4E and Supplementary Figure 6C).

In addition, C57BL/6-NTx-PD-1<sup>-/-</sup> mice older than 4 weeks had hypergammaglobulinemia and significantly increased production of ANAs as detected by ELISA and immunofluorescence assay (Figure 5A-C). All C57BL/6-NTx-PD-1<sup>-/-</sup> mice older than 8 weeks developed AIH, whereas some of the AIH-bearing mice, at a lesser frequency, manifested other organ-specific autoimmunity such as sialadenitis, as did patients with chronic AIH (Figure 5D and Supplementary Table 1).<sup>1-3</sup> These data suggest that chronic AIH in humans and AIH that developed in C57BL/6-NTx-PD-1<sup>-/-</sup> mice share characteristic components of the disease.



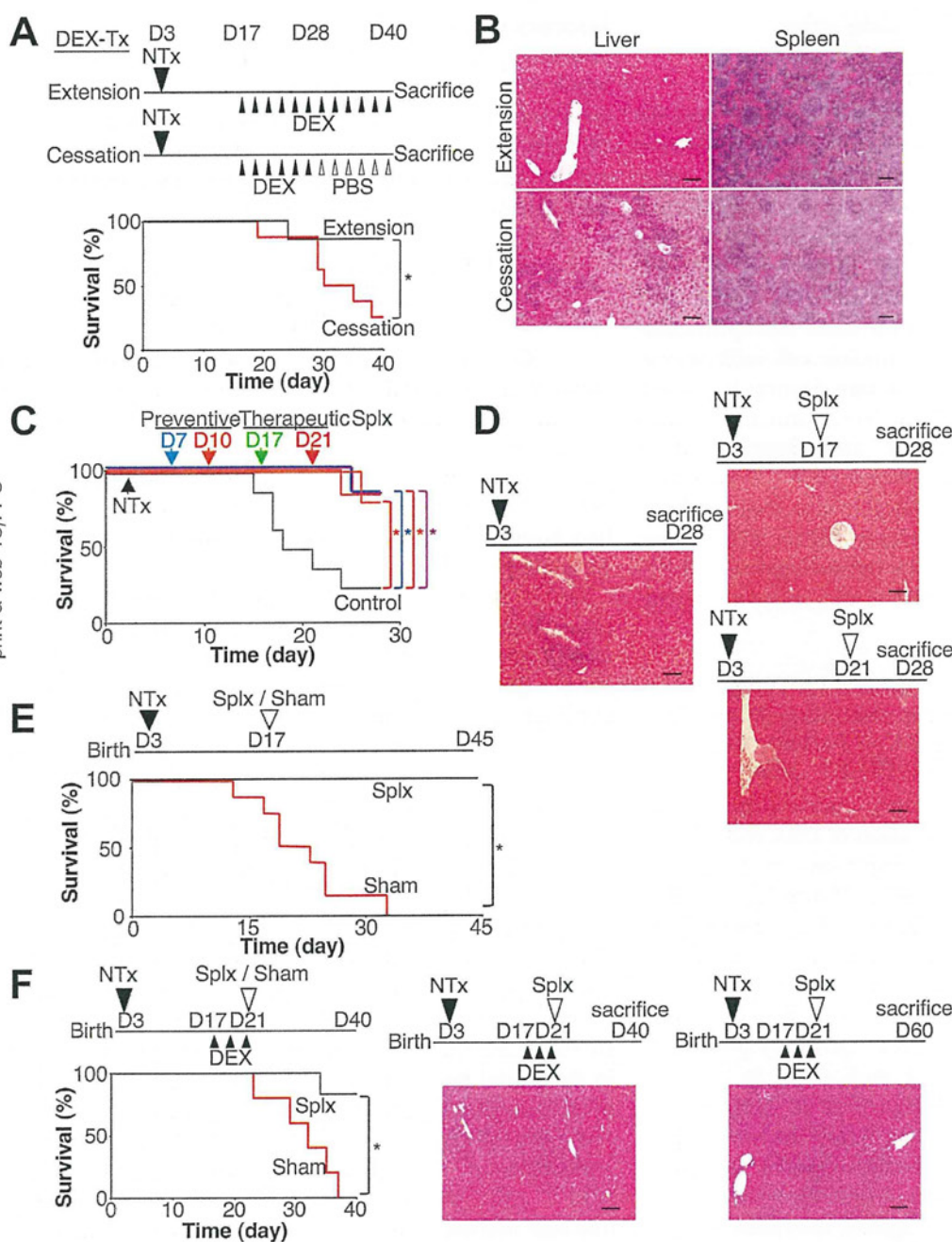


**Figure 3.** Splenectomy overcomes the therapeutic insufficiency of corticosteroids and induces prolonged remission of AIH in BALB/c-NTx-*PD-1*<sup>-/-</sup> mice. (A and B) Mice were treated with DEX therapeutically, as described in Figure 1. Mice that received injections of DEX until 40 days of age (Extension, n = 7) and mice that underwent cessation of DEX injections at 4 weeks of age (Cessation, n = 10) were killed at 40 days of age. (A) Survival rate of each group. (B) Staining of the liver and spleen with H&E. (C and D) Splenectomy (Splx) was performed on BALB/c-NTx-*PD-1*<sup>-/-</sup> mice at 7 (n = 6) or 10 days (n = 5) before induction and 17 (n = 6) or 21 days of age (n = 6) after development of AIH. (C) The survival rate of each group and (D) liver staining with H&E at 28 days of age. (E) The survival rate at 45 days of age in BALB/c-NTx-*PD-1*<sup>-/-</sup> mice undergoing splenectomy (Splx, n = 8) or sham operation (Sham, n = 8) at 17 days of age. (F) Mice were treated with DEX therapeutically, as described in Figure 1. After 3 injections, mice stopped receiving DEX injections and underwent splenectomy (Splx, n = 6) or sham operation (n = 5) at 21 days of age. The survival rate of each group is shown in the left panel. Splx mice were killed at 40 days of age, and the livers were harvested. Liver staining with H&E is shown in the middle panel. For the experiment in F (right panel), indicated mice were killed at 60 days (n = 3). \*P < .05. All scale bars = 100  $\mu$ m.

### Chronic Hepatitis That Developed in C57BL/6-NTx-*PD-1*<sup>-/-</sup> Mice Is Organ-Specific Autoimmunity Induced by CD4<sup>+</sup> T Cells

In 6-week-old C57BL/6-NTx-*PD-1*<sup>-/-</sup> mice, flow cytometric analysis showed that CD3<sup>+</sup> T cells predominantly infiltrated the liver. These cells were mainly CD8<sup>+</sup> T cells and, to a lesser extent, CD4<sup>+</sup> T cells, as described for BALB/c-NTx-*PD-1*<sup>-/-</sup> mice (Figure 5E and F).<sup>11</sup> These results were further confirmed by immunohistology (Figure 6A). In BALB/c-NTx-*PD-1*<sup>-/-</sup> mice, CD4<sup>+</sup> T cells in the enlarged spleen directly triggered development of AIH.<sup>12</sup> Although adult C57BL/6-NTx-*PD-1*<sup>-/-</sup> mice did not show obvious splenomegaly (Figure 6B and

Supplementary Figure 7), transfer of splenic CD4<sup>+</sup> T cells from AIH-bearing C57BL/6-NTx-*PD-1*<sup>-/-</sup> mice at 8 weeks of age into T cell- and B cell-deficient *RAG2*<sup>-/-</sup> mice induced hepatitis in recipient mice at 3 weeks after transfer (Figure 6C). These data suggest that splenic CD4<sup>+</sup> T cells directly trigger AIH in this chronic model.

In addition, using ELISA sets for cytokines, we found that serum cytokine levels of tumor necrosis factor (TNF)- $\alpha$  but not interferon gamma increased in 6-week-old C57BL/6-NTx-*PD-1*<sup>-/-</sup> mice (Figure 6D). Furthermore, when we transferred splenic CD4<sup>+</sup> T cells from AIH-bearing C57BL/6-NTx-*PD-1*<sup>-/-</sup> mice as described previously (Figure 6C), transferred CD4<sup>+</sup> T cells not only induced hepatitis but also elevated serum levels of TNF- $\alpha$



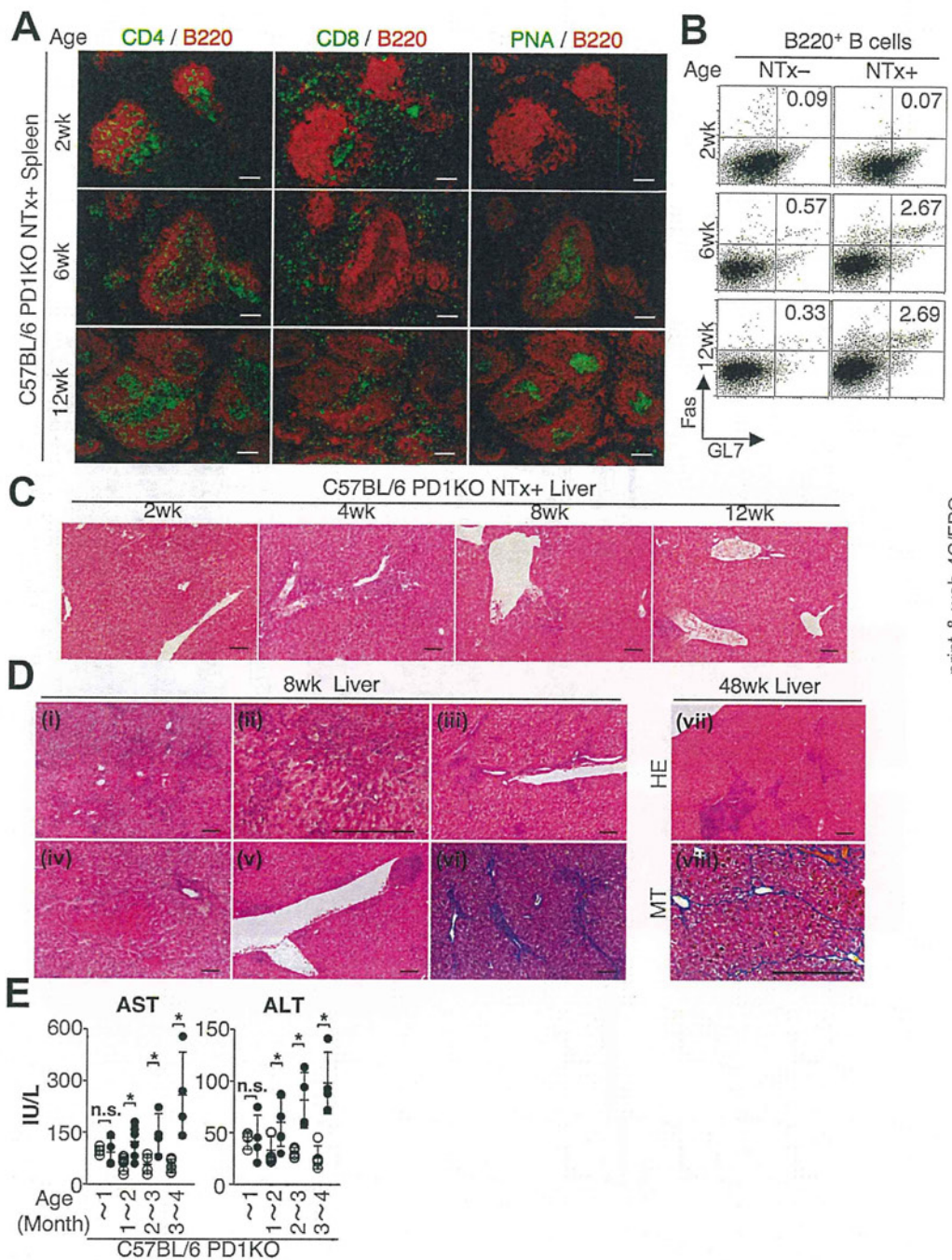


**Figure 4.** Adult C57BL/6-NTx-*PD-1*<sup>-/-</sup> mice spontaneously develop B220<sup>+</sup>PNA<sup>+</sup> GCs in the spleen and have chronic hepatitis with fibrosis. (A) Immunohistological staining of spleens in indicated mice at 2 to 12 weeks. The spleens were stained for CD4, CD8, PNA (green), and B220 (red). (B) Flow cytometric analysis of splenic B cells in indicated mice. The numbers in plots indicate the percentage of B220<sup>+</sup>Fas<sup>+</sup>GL7<sup>+</sup> GC B cells. (C) Liver staining with H&E in C57BL/6-NTx-*PD-1*<sup>-/-</sup> mice at 2 to 12 weeks. (D) Liver staining with H&E for 8-week-old (left panels, i-v) and 48-week-old mice (HE, right panels). Masson's trichrome staining of livers from 8-week-old (left panel, vi) and 48-week-old mice (MT, right panels). (E) Serum levels of AST and ALT in C57BL/6-*PD-1*<sup>-/-</sup> mice at indicated ages with (closed circles) or without NTx (open circles). Bars indicate the mean of each group, and the error bars indicate SD. \**P* < .05. n.s., not significant. All scale bars = 100 μm.

in recipient mice (Figure 6E). Because TNF-α directly and indirectly induces cell death of hepatocytes,<sup>21</sup> TNF-α may be involved in hepatocytic damage in C57BL/6-NTx-*PD-1*<sup>-/-</sup> mice.

Analysis of the T-cell receptor (TCR) repertoire in several autoimmune diseases has shown antigen-driven clonal expansion of autoreactive T cells in the target organs.<sup>22-26</sup> In patients with AIH, analyses of the TCR repertoire have shown skewing of V<sub>β</sub> chain use, suggesting oligoclonal expansion of liver-infiltrating T cells.<sup>27,28</sup> In addition, liver-infiltrating LKM-1-specific CD4<sup>+</sup> T-cell clones have shown a restricted TCR V<sub>β</sub> repertoire.<sup>29</sup> To determine the clonality of infiltrating CD4<sup>+</sup> T cells in the

liver, we used flow cytometry to examine the TCR V<sub>β</sub> use of hepatic CD4<sup>+</sup> T cells. Broad TCR V<sub>β</sub> uses were equivalent to hepatic CD4<sup>+</sup> T cells in wild-type mice and *PD-1*<sup>-/-</sup> mice without NTx (Figure 6F, upper and middle panels). In contrast, in 6-week-old C57BL/6-NTx-*PD-1*<sup>-/-</sup> mice, effector T cells infiltrated into the liver showed clonal expansion (Figure 6F, lower left panel). Interestingly, in the case of fatal hepatitis in 3-week-old BALB/c-NTx-*PD-1*<sup>-/-</sup> mice, effector T cells infiltrated into the liver showed more abundant clonal expansion, probably affecting the severity of inflammation (Figure 6F, lower right panel). These data suggest that monoclonal or oligoclonal expansion of infiltrating effector CD4<sup>+</sup> T cells in Q7



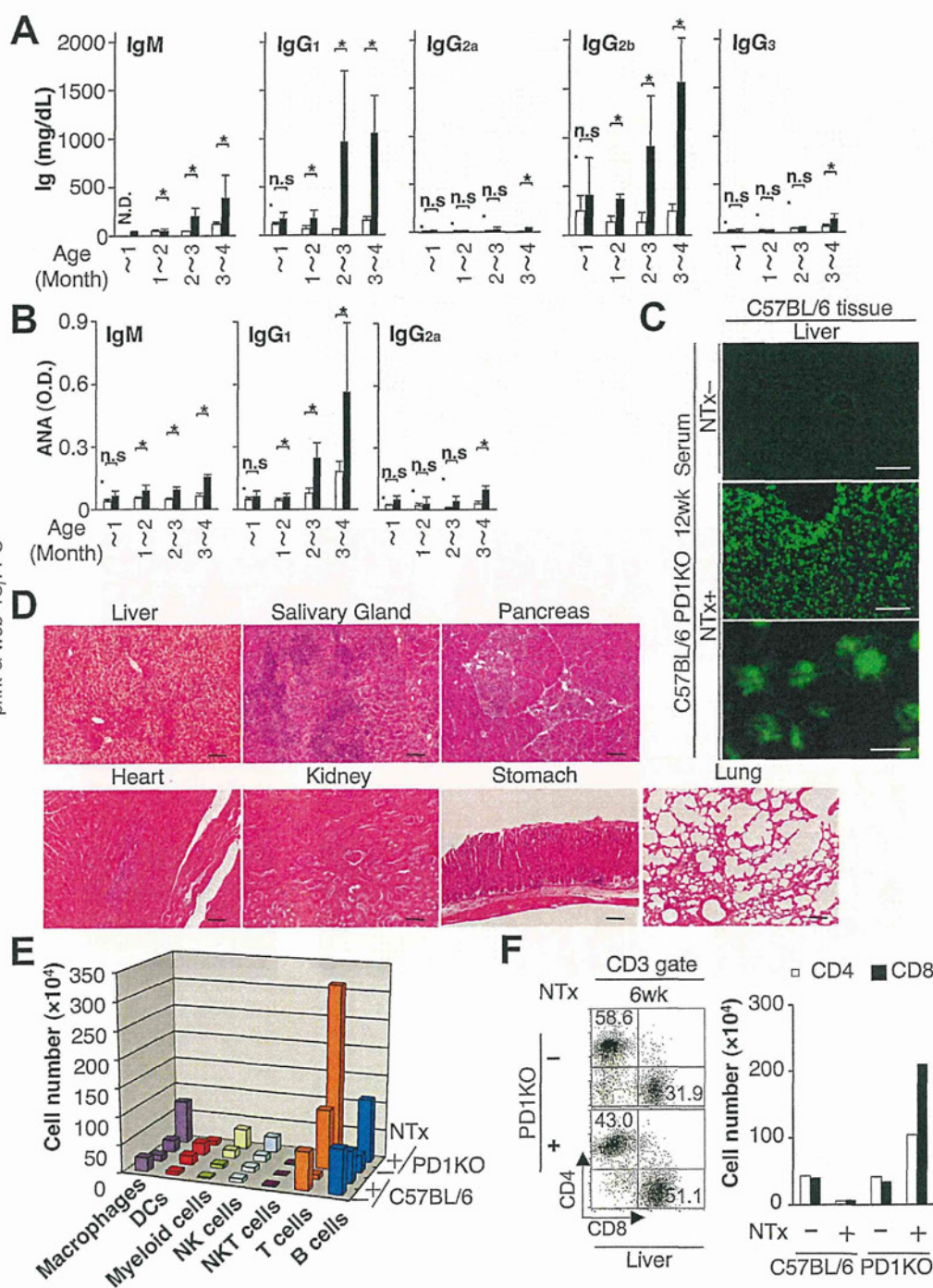


**Figure 5.** Adult C57BL/6-NTx-PD-1<sup>-/-</sup> mice develop hypergammaglobulinemia, ANA production, and autoimmunity in other organs, and T cells are predominantly infiltrated in the inflamed liver. (A and B) The serum levels of (A) total Ig subclasses and (B) ANA subclasses determined by ELISA are shown. Data shown are from C57BL/6-PD-1<sup>-/-</sup> mice at indicated ages with (closed bars) or without NTx (open bars). Bars indicate the mean of each group, and the error bars indicate the SD. \*P < .05. N.D., not detected. n.s., not significant. (C) Autoantibodies detected by fluorescence immunohistology as described in Supplementary Materials and Methods. Sera (100× diluted) from 12-week-old C57BL/6-PD-1<sup>-/-</sup> mice with or without NTx were used. Scale bars = 100 μm (upper and middle panels) or 10 μm (lower panel). (D) Histological findings of various organs from 12-week-old C57BL/6-NTx-PD-1<sup>-/-</sup> mice. Scale bars = 100 μm. (E) Cell numbers of each subset of liver mononuclear cells as described in Supplementary Materials and Methods. Data represent the numbers in the indicated mice at 6 weeks of age. (F) Flow cytometric analysis (left panel) and cell numbers (right panel) of CD3<sup>+</sup>CD4<sup>+</sup> and CD3<sup>+</sup>CD8<sup>+</sup> T cells in the liver of 6-week-old C57BL/6-PD-1<sup>-/-</sup> mice with or without NTx. The numbers in the quadrants indicate the percentage of cells in that gate (left panel). Data shown in C, E, and F are from one of 3 separate experiments.

the liver may be relevant to the proliferation of auto-reactive CD4<sup>+</sup> T cells induced by autoantigen-presenting dendritic cells in the spleen.

In addition, in C57BL/6-NTx-PD-1<sup>-/-</sup> mice, we found that infiltrates in the liver were less likely to contain Tregs (Supplementary Figure 8A). Previously, we showed that in BALB/c-NTx-PD-1<sup>-/-</sup> mice, the transfer of Tregs could not suppress progression of fatal hepatitis after the induction of AIH.<sup>11</sup> However, when Tregs isolated from splenocytes of adult C57BL/6-PD-1<sup>-/-</sup> mice (Supplementary Figure 8B) were transferred into 4-week-old C57BL/6-NTx-PD-1<sup>-/-</sup> mice, the transfer suppressed

chronic AIH (Supplementary Figure 8C-E). In humans, Tregs in peripheral blood have the same suppressive activity as Tregs isolated from the spleen in mice.<sup>30-32</sup> Thus, Tregs isolated from peripheral blood and expanded ex vivo might be able to suppress AIH in humans.

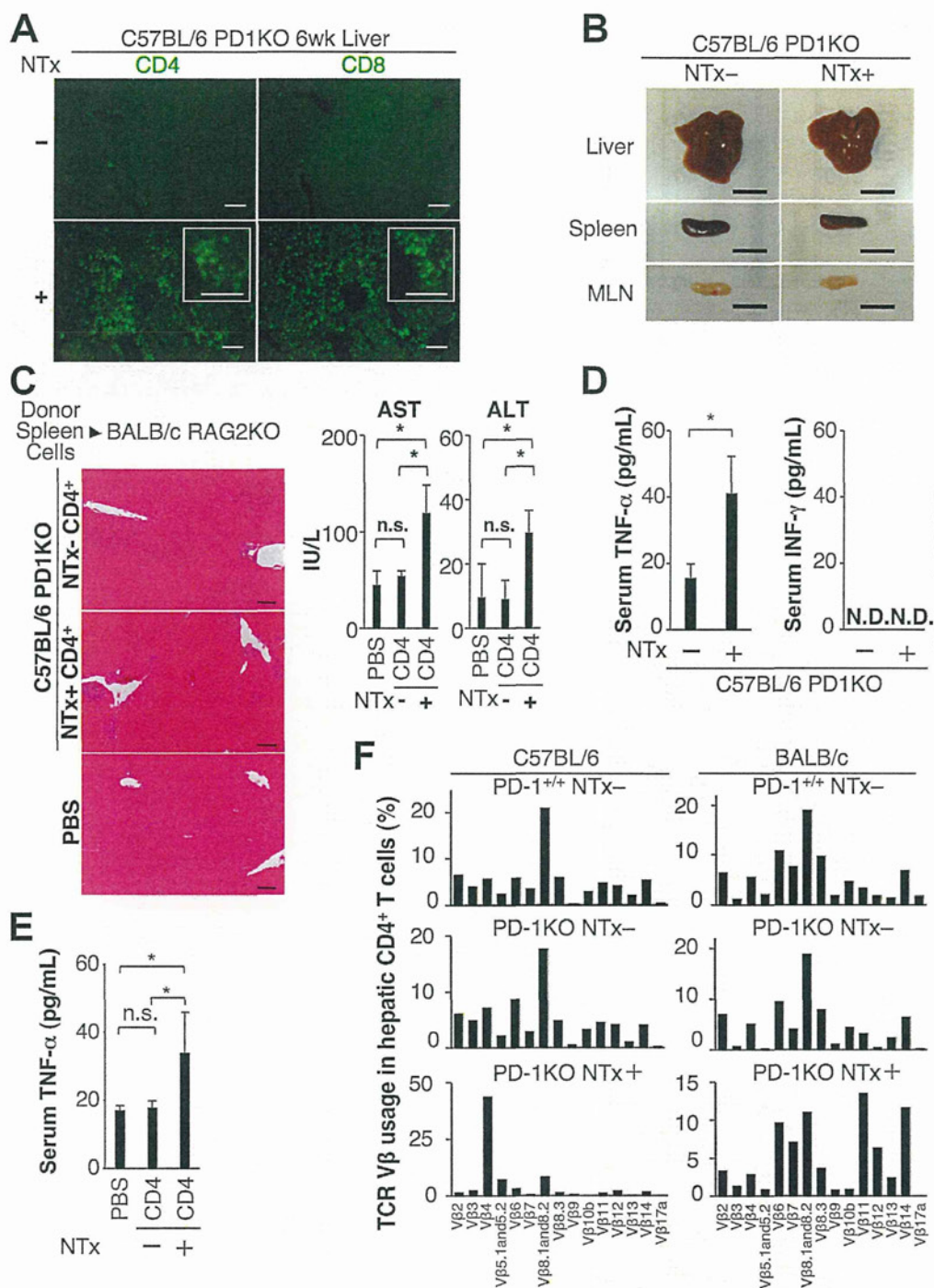
#### The Spleen Is the Induction Site of AIH in C57BL/6-NTx-PD-1<sup>-/-</sup> Mice, and Splenectomy Suppresses Chronic AIH Similar to Fulminant AIH

C57BL/6-NTx-PD-1<sup>-/-</sup> mice at 4 weeks of age showed mononuclear cell infiltrations in the liver and



926  
927  
928  
929  
930  
931  
932  
933  
934  
935  
936  
937  
938  
939  
940  
941  
942  
943  
944  
945  
946  
947  
948  
949  
950  
951  
952  
953  
954  
955  
956  
957  
958  
959  
960  
961  
962  
963  
964  
965  
966  
967  
968  
969  
970  
971  
972  
973  
974  
975  
976  
977  
978  
979  
980  
981  
982  
983

**Figure 6.** Splenic CD4<sup>+</sup> T cells are responsible for induction of chronic AIH, and CD4<sup>+</sup> T cells infiltrated in the liver show clonal expansion in NTx-*PD-1*<sup>-/-</sup> mice. (A) Immunohistological staining of livers. The livers in 6-week-old C57BL/6-*PD-1*<sup>-/-</sup> mice with or without NTx were stained with fluorescein isothiocyanate anti-CD4 or anti-CD8. The insets show staining for CD4 or CD8 with a higher magnification. Scale bars = 100  $\mu$ m. (B) Macroscopic view of the liver, spleen, and mesenteric lymph node (MLN) from 12-week-old indicated mice. Scale bars = 1 cm. (C) Purified CD3<sup>+</sup>CD4<sup>+</sup> T cells from the spleen of 8-week-old C57BL/6-*PD-1*<sup>-/-</sup> mice with or without NTx were transferred into *RAG2*<sup>-/-</sup> mice intravenously. Three weeks after transfer, recipient mice were examined. Liver staining with H&E. Scale bars = 100  $\mu$ m (left panel). Serum levels of the liver transaminases AST and ALT (right panel). (D) Serum levels of TNF- $\alpha$  and interferon gamma (INF- $\gamma$ ) in 6-week-old indicated mice as measured by ELISA. (E) Serum levels of TNF- $\alpha$  in recipient mice transferred as described in C. (F) TCR V $\beta$  uses of hepatic CD4<sup>+</sup> T cells in indicated mice assessed by flow cytometry. Mononuclear cells in the liver were stained as described in Supplementary Materials and Methods. Data shown are from one of 3 separate experiments. The bars in C-E indicate the mean of each group, and the error bars indicate SD. \**P* < .05. n.s., not significant.



984  
985  
986  
987  
988  
989  
990  
991  
992  
993  
994  
995  
996  
997  
998  
999  
1000  
1001  
1002  
1003  
1004  
1005  
1006  
1007  
1008  
1009  
1010  
1011  
1012  
1013  
1014  
1015  
1016  
1017  
1018  
1019  
1020  
1021  
1022  
1023  
1024  
1025  
1026  
1027  
1028  
1029  
1030  
1031  
1032  
1033  
1034  
1035  
1036  
1037  
1038  
1039  
1040  
1041

increased serum levels of AST and ALT (Figures 4C and 7A). To examine whether corticosteroids have therapeutic efficacy for chronic AIH in C57BL/6-NTx-*PD-1*<sup>-/-</sup> mice as in human AIH, intraperitoneal injections of DEX were started at 4 weeks (Figure 7B). After 14 injections every other day until 8 weeks of age, therapeutic injections of DEX suppressed AIH (Figure 7B and Supplementary Figure 9).

As in BALB/c-NTx-*PD-1*<sup>-/-</sup> mice, neonatal splenectomy also suppressed AIH in C57BL/6-NTx-*PD-1*<sup>-/-</sup> mice (Figure 7C and Supplementary Figure 10A and B),

suggesting that the spleen is the induction site for chronic development of AIH in C57BL/6-NTx-*PD-1*<sup>-/-</sup> mice.

Finally, we evaluated splenectomy as a therapeutic option in 4-week-old mice. Similar to the neonatal procedure, splenectomy at 4 weeks suppressed AIH in 8-week-old C57BL/6-NTx-*PD-1*<sup>-/-</sup> mice (Figure 7D and Supplementary Figure 10C and D). Notably, splenectomy neither induced fatal infection nor decreased the survival rate (Supplementary Table 2), whereas splenectomy at 12 weeks suppressed AIH, sustaining remission until 20 weeks of age (Figure 7E and F). Thus, these data



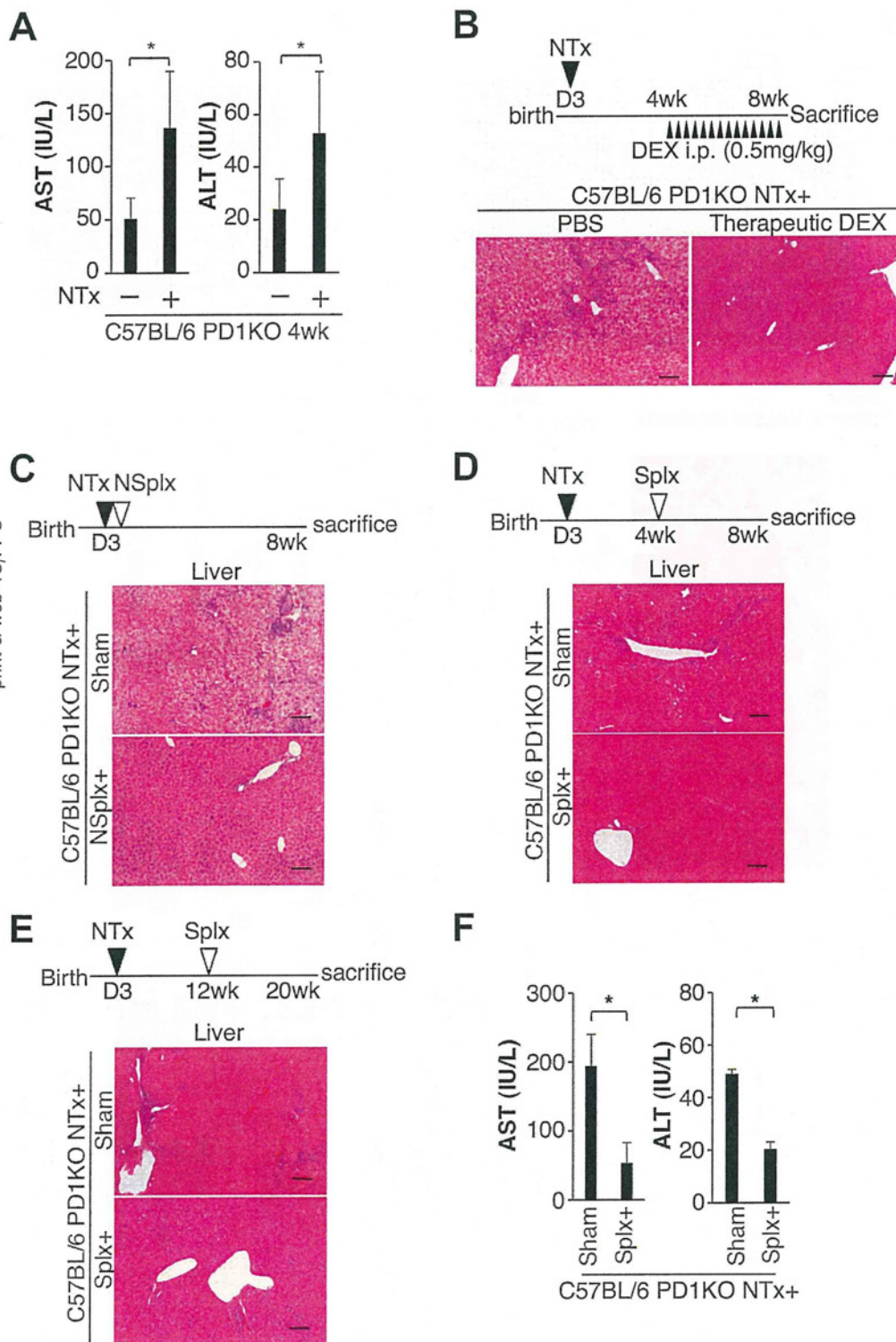


**Figure 7.** C57BL/6-NTx-*PD-1*<sup>-/-</sup> mice at 4 weeks of age show increased serum levels of the liver transaminases, and therapeutic injections of DEX as well as splenectomy suppress chronic AIH. (A) Serum levels of the liver transaminases AST and ALT in 4-week-old indicated mice. (B) Intraperitoneal injections of DEX (n = 5) or PBS (n = 5) were started at 4 weeks. After 14 injections every other day until 8 weeks of age, mice were killed and examined. (C) Mice underwent a splenectomy (NSplx, n = 5) or a sham operation (n = 5) at 1 day after NTx and were analyzed at 8 weeks. (D) Four-week-old mice underwent a splenectomy (Splx, n = 5) or a sham operation (n = 5) and were analyzed at 8 weeks. (E and F) Twelve-week-old mice underwent a splenectomy (Splx, n = 5) or a sham operation (n = 5) and were analyzed at 20 weeks. (B–E) Liver staining with H&E and (A and F) serum levels of AST and ALT. Bars indicate the mean of each group, and the error bars indicate SD. \**P* < .05. n.s., not significant. Scale bars = 100  $\mu$ m.

suggest that splenectomy has therapeutic efficacy for chronic AIH similar to fulminant AIH.

## Discussion

Using the AIH models, we here examined the effects of treatment with DEX to find clues to overcoming therapeutic insufficiency of corticosteroids for AIH. We

showed that T<sub>FH</sub> cells in the spleen are responsible not only for the development of AIH but also for relapse after discontinuing treatment with corticosteroids. In BALB/c-NTx-*PD-1*<sup>-/-</sup> mice, the spleen is the induction site for fatal AIH, and responsible T<sub>FH</sub> cells are dysregulated in the spleen under the concurrent loss of Tregs and PD-1-mediated signaling. CCR6-CCL20 axis-dependent migration of these T cells triggers AIH.<sup>12</sup> In addition,



fatal progression is mediated by further differentiation of Th1-type effector T cells from  $T_{FH}$  cells in the spleen, and a specific chemokine-dependent migration of those T cells is crucial for fatal progression (unpublished data). We showed that injections of DEX are therapeutic for fatal AIH in this model whereas  $T_{FH}$  cells still exist in the spleen even after continuous administration of DEX; discontinuing treatment resulted in fatal AIH. In addition, residual splenic  $CD4^+$  T cells were more resistant to DEX-mediated apoptosis after therapeutic injections of DEX, and transfer of these residual splenic  $CD4^+$  cells induced the development of hepatitis in the recipient  $RAG2^{-/-}$  mice. From these data, we concluded that in the mouse model of AIH, corticosteroid therapy has the drawback of allowing dysregulated  $T_{FH}$  cells to remain in the spleen.

We described another AIH model in which C57BL/6-NTx-PD-1<sup>-/-</sup> mice developed chronic hepatitis with fibrosis, hypergammaglobulinemia, and the production of ANA. Notably, dysregulated  $T_{FH}$  cells were generated in the spleen, neonatal splenectomy suppressed chronic AIH, and transfer of splenic  $CD4^+$  T cells induced hepatitis in the recipient  $RAG2^{-/-}$  mice. These results indicate that the same induction mechanisms are involved in the development of AIH in mice, with manifestations ranging from acute onset to chronic. In humans, it is unknown at present whether the spleen is the induction site of AIH or whether  $T_{FH}$  cells are responsible for the development of AIH, although splenomegaly is a common clinical finding in patients with active AIH.<sup>1-3</sup> Therefore, it is important to know whether similar mechanisms are involved in the relapse of AIH in humans after withdrawal of corticosteroids.

In our previous and present studies, we showed that splenectomy, either neonatal or at 7 or 10 days of age before the induction of AIH, suppressed AIH presenting as fulminant hepatic failure in BALB/c-NTx-PD-1<sup>-/-</sup> mice.<sup>12</sup> In this study, we revealed that neonatal splenectomy also suppressed the development of chronic AIH in C57BL/6-NTx-PD-1<sup>-/-</sup> mice. Because patients with severe AIH have a high potential for recurrence after liver transplantation, leading to a greater probability of graft loss, splenectomy might well prevent such recurrence.

Interestingly, we further observed in this study that splenectomy after the development of AIH suppressed liver inflammation with manifestations ranging from acute onset to chronic. In the acute AIH model, splenectomy alone suppressed liver inflammation and sustained remission for 4 weeks. In addition, splenectomy after treatment with DEX suppressed AIH and extended remission beyond 4 weeks. Moreover, in the chronic AIH model, splenectomy at 12 weeks of age suppressed AIH, sustaining remission until 20 weeks. It is well known that patients with AIH in remission after withdrawal of corticosteroid therapy are likely to experience a relapse and that multiple relapses are associated with poor prognosis.<sup>7,8</sup> Therefore, it is of interest to determine whether splenectomy might be considered in some patients with

AIH, although this will need to be very carefully assessed given the concerns related to splenectomy.

In conclusion, we showed that although corticosteroid therapy has therapeutic efficacy for AIH in mice, it allows residual splenic dysregulated  $T_{FH}$  cells to remain after treatment, which appear to be responsible for relapse. In addition, we found that splenectomy overcomes this insufficiency, inducing prolonged remission of AIH. These data may prove useful in obtaining complete remission in humans with AIH.

### Supplementary Material

Note: To access the supplementary material accompanying this article, visit the online version of *Gastroenterology* at [www.gastrojournal.org](http://www.gastrojournal.org), and at <http://dx.doi.org/10.1053/j.gastro.2013.03.011>

### References

- Krawitt EL. Autoimmune hepatitis. *N Engl J Med* 2006;354:54-66.
- Manns MP, Czaja AJ, Gorham JD, et al. Diagnosis and management of autoimmune hepatitis. *Hepatology* 2010;51:2193-2213.
- Czaja AJ, Manns MP. Advances in the diagnosis, pathogenesis, and management of autoimmune hepatitis. *Gastroenterology* 2010;139:58-72.
- Manns MP. Autoimmune hepatitis: the dilemma of rare diseases. *Gastroenterology* 2011;140:1874-1876.
- Czaja AJ, Davis GL, Ludwig J, et al. Complete resolution of inflammatory activity following corticosteroid treatment of HBsAg-negative chronic active hepatitis. *Hepatology* 1984;4:622-627.
- Czaja AJ. Safety issues in the management of autoimmune hepatitis. *Expert Opin Drug Saf* 2008;7:319-333.
- Czaja AJ, Ammon HV, Summerskill WH. Clinical features and prognosis of severe chronic active liver disease (CALD) after corticosteroid-induced remission. *Gastroenterology* 1980;78:518-523.
- Montano-Loza AJ, Carpenter HA, Czaja AJ. Consequences of treatment withdrawal in type 1 autoimmune hepatitis. *Liver Int* 2007;27:507-515.
- Montano-Loza AJ, Carpenter HA, Czaja AJ. Improving the end point of corticosteroid therapy in type 1 autoimmune hepatitis to reduce the frequency of relapse. *Am J Gastroenterol* 2007;102:1005-1012.
- Hoeroldt B, McFarlane E, Dube A, et al. Long-term outcomes of patients with autoimmune hepatitis managed at a nontransplant center. *Gastroenterology* 2011;140:1980-1989.
- Kido M, Watanabe N, Okazaki T, et al. Fatal autoimmune hepatitis induced by concurrent loss of naturally arising regulatory T cells and PD-1-mediated signaling. *Gastroenterology* 2008;135:1333-1343.
- Aoki N, Kido M, Iwamoto S, et al. Dysregulated generation of follicular helper T cells in the spleen triggers fatal autoimmune hepatitis in mice. *Gastroenterology* 2011;140:1322-1333.
- King C. New insights into the differentiation and function of T follicular helper cells. *Nat Rev Immunol* 2009;9:757-766.
- Knodell RG, Ishak KG, Black WC, et al. Formulation and application of a numerical scoring system for assessing histological activity in asymptomatic chronic active hepatitis. *Hepatology* 1981;1:431-435.
- Wyllie AH. Glucocorticoid-induced thymocyte apoptosis is associated with endogenous endonuclease activation. *Nature* 1980;284:555-556.
- Compton MM, Cidlowski JA. Rapid in vivo effects of glucocorticoids on the integrity of rat lymphocyte genomic deoxyribonucleic acid. *Endocrinology* 1986;118:38-45.
- Chen X, Murakami T, Oppenheim JJ, et al. Differential response of murine  $CD4^+CD25^+$  and  $CD4^+CD25^-$  T cells to dexamethasone-induced cell death. *Eur J Immunol* 2004;34:859-869.
- Czaja AJ, Carpenter HA, Santrach PJ, et al. Significance of HLA DR4 in type 1 autoimmune hepatitis. *Gastroenterology* 1993;105:1502-1507.